Cite this article as:

López J., Battaglia G., Lupo D., Fernández de Labastida M., Vallès V., Luis Cortina J., Cipollina A., Micale G., Integration of ion-exchange and crystallisation processes to recover boric acid and magnesium hydroxide from saltworks bitterns, *Separation and Purification Technology*, Volume 354, Part 8, 19 February 2025, 129532.

https://doi.org/10.1016/j.seppur.2024.129532

Pre-print version of

Integration of ion-exchange and crystallisation processes to recover boric acid and magnesium hydroxide from saltworks bitterns

Julio López[1,2,*,†], Giuseppe Battaglia[3,**, †], Dario Lupo[3], Marc Fernández de Labastida[1,2], Víctor Vallès[1,2], Jose Luis Cortina[1,2,4], Andrea Cipollina[3], Giorgio Micale[3]

[1] *Chemical Engineering Department, Escola d'Enginyeria de Barcelona Est (EEBE), Universitat Politècnica de Catalunya (UPC)-BarcelonaTECH, C/ Eduard Maristany 10-14, Campus Diagonal-Besòs, 08930 Barcelona, Spain*

[2] *Barcelona Research Center for Multiscale Science and Engineering, Campus Diagonal-Besòs, 08930 Barcelona, Spain*

[3] *Dipartimento di Ingegneria, Università degli Studi di Palermo (UNIPA), Viale delle Scienze, 90128 Palermo, Italy*

[4] *CETaqua, Carretera d'Esplugues, 75, 08940 Cornellà de Llobregat, Spain*

* julio.lopez.rodriguez@upc.edu

** giuseppe.battaglia03@unipa.it

† These authors contributed equally to this work.

23 **GRAPHICAL ABSTRACT**

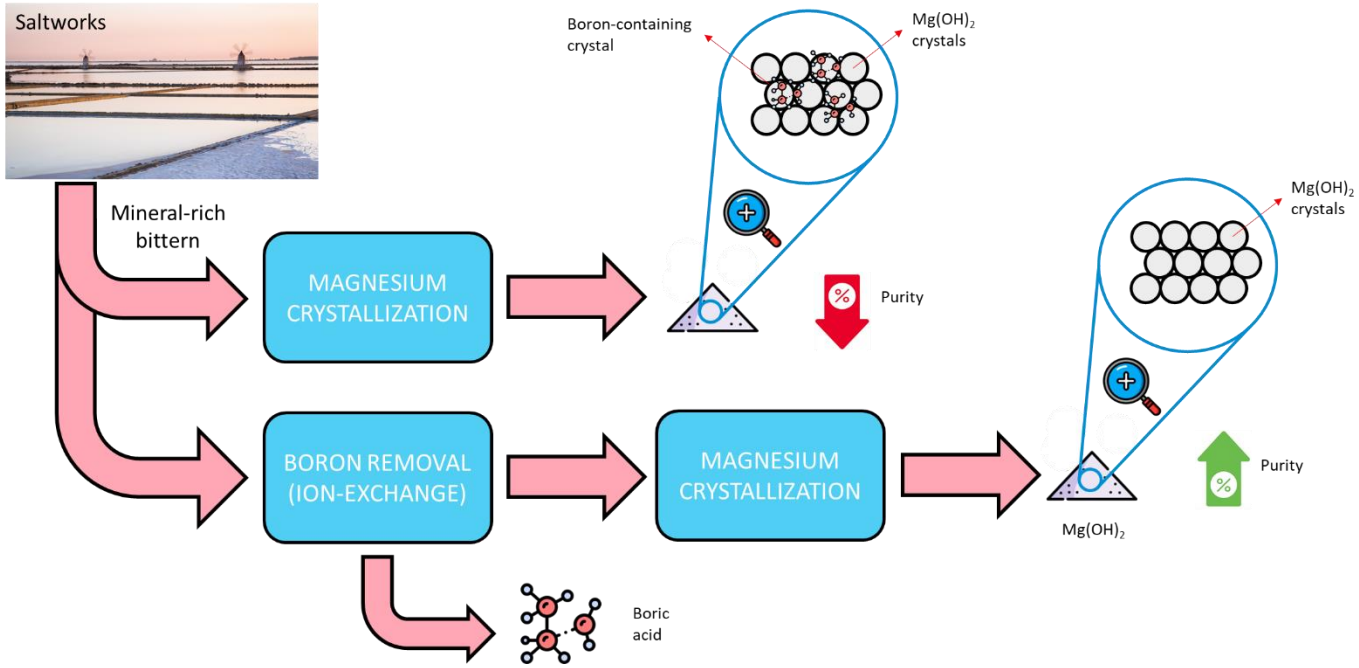

24

25

LIST OF ABBREVIATIONS

BE	Backscattered Electrons
CRMs	Critical Raw Materials
CF	Concentration factor
EU	European Union
FESEM-EDS	Field Emission Scanning Electron Microscopy Energy Dispersive X-ray Spectroscopy
ICP-MS	Inductively Coupled Plasma Mass Spectrometry
ICP-OES	Inductively Coupled Plasma Optical Emission Spectroscopy
PV	Pore volume
PVC	Polyvinyl chloride
q	Resin capacity
RP	Recovery percentage
SEI	Secondary Electron Imaging
TEs	Trace Elements
TG	Thermogravimetric analysis
XRD	X-ray diffraction

ABSTRACT

The lack of primary sources of the so-called Critical Raw Materials within the European Union is directing research towards alternative mining to extract them. Among the different potential alternative sources, the brines generated in traditional saltworks (denominated *bitterns*) can be a very promising option. In fact, several elements can be up to 50 times more concentrated in bitterns than in seawater. Magnesium, for example, can present concentrations above 50 g/L, and its recovery can be pursued as hydroxide by using crystallization processes. However, the presence of boron even at relatively low concentrations (100 mg/L – 150 mg/L) can contaminate the final magnesium hydroxide, thus making it not suitable for certain applications, such as the refractory industry (target <~ 0.11 mg B/g of magnesium hydroxide). Because of boron speciation (as boric acid), only chelating ion-exchange resins based on N-methylglucamine functional groups can selectively remove boron from aqueous solutions. In this work, the integration of ion-exchange and crystallization processes is carried out to produce pure magnesium hydroxide from real *bitterns* collected in Trapani (Sicily). Two different bitterns were treated with two commercial B-selective chelating ion-exchange resins (S108 and CRB05), and the boron-free bittern was later used for $Mg(OH)_2$(s) crystallization. The effect of pH on $Mg(OH)_2$(s) crystallization was studied and data was compared (in terms of purity) in the cases with or without B-removal pre-treatment. Moreover, once the resin was saturated, elution with HCl allowed to recover H_3BO_3 via evaporative crystallization. Results showed the possibility of recovering pure $Mg(OH)_2$(s) (>98%) with low B-content (<0.10 mg B/g), matching the specifications for refractory industry, and H_3BO_3 with 95% purity.

KEYWORDS: Brine valorisation; Minerals recovery; magnesium hydroxide; chelating resins; N-methylglucamine; precipitation.

1. Introduction

The first list of Critical Raw Materials (CRMs), including 14 elements and minerals, was presented by the European Union (EU) in 2011. These materials have attracted a growing concern due to their supply risk and economic importance. The list of CRMs has been reviewed several times, and in its last version, released in 2023, it includes up to 34 CRMs [1]. Boron (B) and Magnesium (Mg) have been included among the CRMs since the first list [2].

Seawater has emerged as a promising alternative source for recovering critical elements through sea mining, as its composition covers nearly every element in the periodic table [3,4]. However, most of these elements exist in seawater at concentrations of a few mg/L, or even below, being in fact called Trace Elements (TEs) [5]. It has been demonstrated that only the most concentrated components in seawater (i.e. Na, K, Mg, Cl) can be extracted through economically viable approaches [6–8]. Conversely, the feasibility of recovering TEs from seawater is compromised by the energy-intensive extraction processes involved [9,10].

In this context, concentrated brines are promising alternatives to explore. EU is investing, through sea mining, towards the extraction of various raw materials, critical or not, from concentrated brines from either (i) desalination plants or (ii) seawater solar saltworks, as in the case of the EU-funded project SEArcularMINE [11]. In the latter scenario, brine is originated in *saltworks*, which are extensive areas where seawater fills shallow ponds. Here, solar and wind action cause seawater to evaporate and concentrate, leading to the crystallization of calcium compounds, first, and sea salt (NaCl) eventually [12,13]. The mother liquor remaining after salt crystallisation, known as *bittern*, becomes significantly concentrated (20 to 50 times more than seawater for some elements) and devoid of Ca. For instance, in Trapani (Italy), Vicari et al. [14] performed the characterization of bittern in saltworks ponds. The authors evaluated the composition along the ponds and reported that Mg and B concentrations increased from 1480 mg/L and 4.5 mg/L (in seawater) to 22000 mg/L and 79 mg/L (in bittern), respectively. Randazzo et al. [15] provided a more extensive characterization of different *bitterns* along the Mediterranean basins from different sources, showing that final composition depends on the collecting period and production process. Authors reported concentrations up to 75 g/L Mg and 400 mg/L B. The high B and Mg concentrations in bitterns could offer a viable alternative route for these element-based compounds production, especially considering that 98% of Europe's demand for B in the form of borates is currently provided by Turkey, whereas 97% of the European demand for Mg is provided by China [16].

Different methods are reported in the literature for recovering B from aqueous saline solutions [17–19], including evaporation-crystallisation, precipitation-coagulation, ion exchange or membrane technologies, such as reverse osmosis or electrodialysis. However, B separation is challenging with the latter option as, in aqueous solution, B can be found as boric acid or borate ion, depending on the solution pH (pK_a(25ºC) = 8.76) [18].

N-methylglucamine resins have been widely studied for B removal and/or recovery from aqueous streams [20–23], including brines [24–26], as they have higher selectivity towards B than other ion exchange resins and they can be regenerated with strong acids as sulphuric and hydrochloric [27]. The Diaion CRB03 and CRB05 (Mitsubishi Chemical Corporation), S108 (Purolite) or Amberlite IRA743 (Dupont) are commercially available examples of macroporous styrene-divinyl benzene resins containing N-methylglucamine functional groups. Excluding the latter one, Figueira et al. [26] applied these resins for recovering B from seawater RO brines at pH 5.9, reporting that Langmuir maximum adsorption capacities were 10.9, 12.9 and 16.6 mg_B/g for S108, CRB05 and CRB03, respectively. However, the use of N-methylglucamine resins for the specific treatment of solar saltworks bitterns has not been extensively studied yet. Up to 30 sorbents, including different functional groups, were evaluated in batch mode by Vallès et al. [28] concluding that, apart from B, N-methylglucamine resins presented also high affinity for Ga, Ge and Co. Recently, the same authors have evaluated three B-selective resins (Purolite S108, Diaion CRB03 and Diaion CRB05) in column mode aiming to recover B, Co, Ga and Ge from synthetic bitterns mimicking different real scenarios [29]. In that study, an adsorption capacity of 8.3 mg_B/g for S108 and 11 mg_B/g for both CRB03 and CRB05 was reported, being normally able to recover >90% of the B retained by the resins.

After B extraction by the chelating resins, it can be recovered in an elution step with HCl solutions. In these streams, B concentration can increase up to 15 times more than in the treated bittern [26,29]. Consequently, a precipitation stage could be applied in order to recover B as a solid. B could be precipitated as borate or boric acid, or by coagulation using $AlCl_3$ or $FeCl_3$ [30], typically with low B concentrations (e.g. 120 mg/L). However, a large quantity of chemicals is required and a huge amount of sludge is generated [31]. When treating solutions with higher B contents (e.g. 4.1 g/L), precipitation in the form of $Ca_2B_2O_5 \cdot H_2O$ (parasibirskite) using $Ca(OH)_2$ is preferred [32]. Alternatively, H_3BO_3 could be crystallised by evaporation [33,34]. This procedure was successfully applied to a multi-component solution containing 1.8 g_B/L, in which 76% of B was recovered after evaporating 90% of the water at 70 °C [35].

Boron extraction from saline solutions is desirable also if high-purity Mg is going to be recovered from the same stream. Mg has been successfully recovered from bittern in the form of magnesium hydroxide, $Mg(OH)_2(s)$, by the addition of alkaline reactants [36]. $Mg(OH)_2(s)$ is a white odourless compound, extensively employed in numerous industrial fields, e.g. as neutralising and antibacterial agent in wastewater treatment, primary raw material for the refractory industry, nontoxic flame retardant filler in polymeric materials [37]. The impact of boron content in $Mg(OH)_2$ powders has been widely discussed in the scientific and patent literature. For example, it has been reported that, the maximum equivalent boron oxide, B_2O_3, content must be lower than 1 mg B_2O_3/g-MgO on the ignited basis, i.e. namely referred to the magnesium oxide (MgO) compound, thus being ~0.11 mg B/g-$Mg(OH)_2(s)$, for solids applicability in the refractory sector [38]. In 1985, Spoors et al. [39] presented a treatment process scheme for seawater brines or aqueous Mg-containing solutions based on the use of adsorptive magnesium hydroxide to remove boron species and increase $Mg(OH)_2(s)$ purity. The brine was mixed with adsorptive magnesium hydroxide solids in a series of counter-current stages. Some years later, Wilkomirsky et al. [40] proposed the addition of hydrochloric acid to the saline solutions to precipitate boron as boric acid. Li et al., [41] investigated the possible use of chelating resins (e.g.Purolite S108) for the adsorption of boron from the residual brines of Chinese salt lakes with the aim to prepare boron-free magnesia compounds. Recently, Bonin et al. [42] treated lithium-rich brines through Amberlite IRA743 resins. The pre-treatment successfully reduced the boron content in the brine leading to (i) a decrease of the brine loss caused by mother liquor intake in $Mg(OH)_2$ solids and (ii) an increase of the purity of synthesized $Mg(OH)_2(s)$ products.

In the present work, the proposed process aims to integrate B-selective chelating resins and crystallization processes to demonstrate the technical feasibility of recovering high purity products from *bitterns*. Several operation conditions were explored, aiming at improving the purity of the $Mg(OH)_2(s)$ recovered with the objective to make it suitable for the refractory industry (<~0.11 mg B/g-$Mg(OH)_2(s)$). In the experimental campaign, different resins were evaluated for boron and germanium, whereas for $Mg(OH)_2(s)$ crystallization, the effect of final pH was studied. The results achieved showed that by integrating these two technologies it was possible to recover highly pure boric acid and magnesium hydroxide, the latter one characterized by a low boron concentration.

2. Material and Methods

Figure 1 shows a block flow diagram of the investigated bittern treatment chain for the simultaneous recovery of boron (as boric acid) and magnesium (as magnesium hydroxide) from real saltworks bitterns.

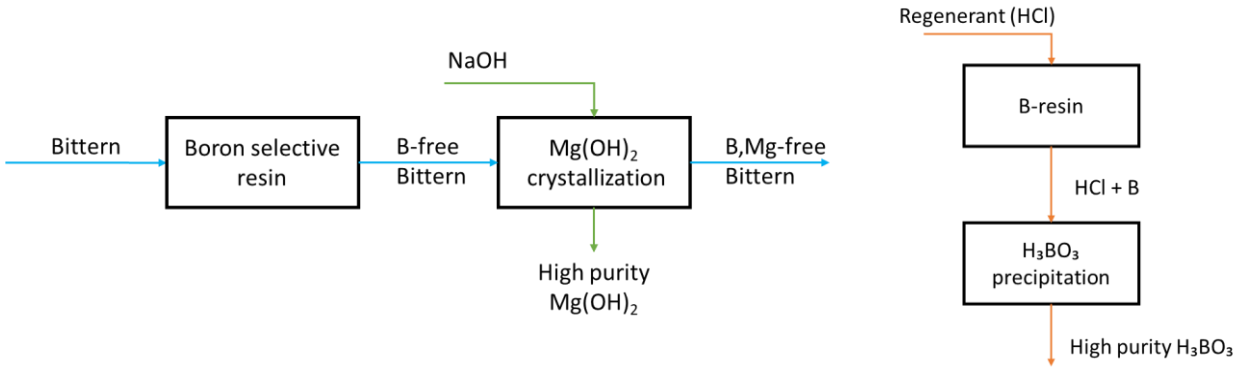

(a) (b)

Figure 1 *Bittern treatment steps for the production of high purity (a) $Mg(OH)_2$(s) and (b) H_3BO_3(s) from the eluate.*

In order to recover pure $Mg(OH)_2$(s), ion exchange resins are first adopted to extract boron directly from the bittern generated at the solar saltworks (see Figure 1.a). B-selective chelating resins were employed to capture and concentrate B from bitterns in a sorption-desorption cycle. Specifically, the performances of two commercial resins (e.g. S108 and CRB05), were investigated by treating two real bitterns collected from Margi and Galia saltworks, both located in the district of Trapani, Italy. The boron-free bittern is further treated with sodium hydroxide (NaOH) solutions to precipitate Mg ions in the form of $Mg(OH)_2$(s). The solids were precipitated from treated and untreated bitterns at two final pH values of 10.8 (stoichiometric conditions) and 12 (alkaline excess) with NaOH solutions. Following boron breakthrough (see Figure 1.b), a regenerant aqueous HCl solution is employed to extract the boron from the resins before using an evaporation-crystallisation method to recover boric acid (H_3BO_3(s)).

2.1. Solutions and Chemicals

Two real bitterns, collected from Margi and Galia saltworks (Trapani, Italy), were employed in the experimental campaign. Table 1 presents their composition in terms of major and minor elements.

Table 1 *Margi and Galia bitterns composition assessed via Ion Chromatography (IC), Inductively Coupled Plasma Optical Emission Spectrometry (ICP-OES) and Inductively Coupled Plasma Mass Spectrometry (ICP-MS) techniques.*

Analytical Technique		Margi	Galia
IC	Na^+	54190	67638
(mg/L)	K^+	12749	10532
	Cl^-	185405	180149
	Br^-	2084	1573
	$^*SO_4^{2-}$	60799	45663
ICP-OES	B	161.2	133.3
(mg/L)	Ca	142.9	157.7
	Mg	49551	37499
	$^{**}S$	24131	18516
	K	-	-
ICP-MS	Li	7519	5801
(µg/L)	Co	< 10	< 10
	Ga	< 25	< 25
	Ge	< 10	< 10
	Rb	4083	3283
	Sr	12004	25611
	Cs	4.78	2.59

* SO_4^{2-} refers to sulphate ions measured by IC
** S refers to total elemental sulphur measured by ICP-OES

NaOH solutions were prepared by dissolving pellets of analytical grade (Honeywell|Fluka™, with a purity of >98 %) in deionized water. NaOH solution concentrations were checked via titration by

adopting a standard HCl solution. 1 M HCl solutions were obtained from 37 % wt HCl solution (Honeywell) diluted in deionized water.

2.2. Experimental set-up and procedure

2.2.1. Boron adsorption and resin regeneration

Two different resins were employed to recover boron: Purolite® S108 and Mitsubishi DIAION CRB05. Both resins present the same chemistry, based on N-methylglucamine functional groups, but differing in particle size, density and capacity (see Table 2).

Table 2 *Main properties of the N-methylglucamine sorbents used in this study.*

Sorbent (abbreviation)	Supplier	Ionic form	Capacity (eq/L)	Humidity content (%)	Particle size (mm)	Density (g/L)	Ref.
Purolite S108 (S108)	Purolite	F.B.	0.60	61-67	0.43-0.63	670-730	[43]
Diaion CRB05 (CRB05)	Mitsubishi Chemical	F.B.	0.95	45-53	0.55	750	[44]

F.B.: free base

Based on the resin functional groups, the complexation mechanism between of boron follows the reaction shown in Figure 2 [28]

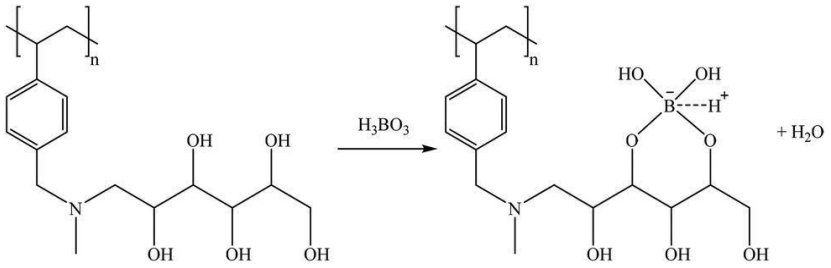

Figure 2 *Complexation mechanism leading the formation of monoborate complex in the adopted functionalized resins* [28]

Resins were packed in a polyvinyl chloride (PVC) column of 49.7 cm length, with an inner diameter of 2.7 cm. 75% of the column volume was occupied with the resin (c.a. 128 g of resin), leaving the rest un-occupied to account for resin expansion during acid regeneration. At the top and bottom of the column glass fiber was allocated. Figure 3 shows a picture and a schematic representation of the experimental set-up. The brine was fed from the feed tank to the bottom of the column by using a KRONOS 50 peristaltic pump, which was manually adjusted to the desired flow-rate. At the outlet of the column, another tank was placed to collect the treated bittern for carrying out $Mg(OH)_2(s)$ crystallization tests. Samples were periodically collected at the outlet of the column to be analyzed.

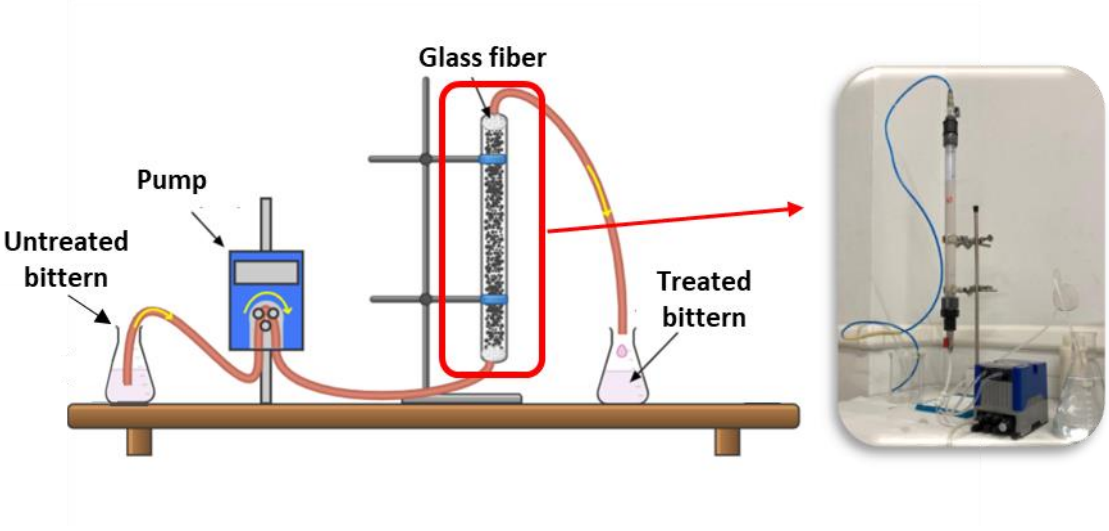

(a) (b)

Figure 3 *(a) Schematic representation of the experimental set-up employed for the boron removal step from real saltworks bittern. (b) A picture of the experimental set-up.*

Before starting the experimental campaign, and once the resin was packed, the pore volume of the column was measured. To do that, 0.05 M NaCl was circulated across the experimental set-up at 10 mL/min and the conductivity of the outlet solution was measured to determine the residence time and, therefore, the pore volume.

Each experimental test consisted of: (i) bittern feeding the column and relevant saturation in boron (ii) displacement of the bittern inside the column with distilled water, (iii) boron elution from the resin using 1 M HCl, and (iv) displacement of HCl with water before starting another cycle. It must be highlighted that resin operation was carried out using the H^+ form, rather than in the Na^+ form to avoid NaCl(s) precipitation inside the column.

Analyzing the B-content in the outlet samples, breakthrough curves were obtained and plotted, whereas during regeneration, the elution profiles were determined. The data collected was used to calculate the resin capacity (q, mg/g resin), the concentration factor (CF, dimensionless) and the recovery percentage (RP, %). The resin capacity (Eq. 1) accounts for the amount of boron that was sorbed per gram of resin, while the CF (Eq. 2) is used to express how much boron was concentrated in the eluate with respect to the feed:

$$q = C_0 \frac{\int_0^V \left(1 - \frac{C}{C_0}\right) dV}{m_{resin}} \quad (1)$$

$$CF = \frac{\frac{1}{V_{el}} \int_0^{Vel} C \, dV}{C_0} \quad (2)$$

Where C_0 is the initial concentration of the species in the brine (mg/L), V is the volume of brine that circulated through the column (L), $m_{resin}$is the mass of resin (g), C is the concentration of the species at the exit of the column (mg/L), and V_{el} is the volume of solution used during the elution (L).

Finally, the RP, used to assess if the resin was completely regenerated, is calculated according to Eq. 3:

$$RP = \frac{\int_0^{Vel} C dV}{q \cdot m_{resin}} \cdot 100 \quad (3)$$

Four different tests were performed for the boron removal step, varying type of bittern, adopted resin and flow rate, as illustrated in Table 3. Initially, the Margi bittern was tested with the two resins with the objective to evaluate resins performance toward boron and possible other element extraction (namely tests MP1 and MD1). During these tests, the brine was fed at a flow rate of 2 PV/h (11.4 mL/min for the Purolite S108 and 10.7 mL/min for Diaion CRB05). Following saturation, desorption was carried out at 0.5 PV/h (2.85 mL/min for the Purolite S108 and 2.67 mL/min for Diaion CRB05). Considering that Purolite S108 was the only one able to extract both B and Ge, it was later used to treat the Galia bittern. In this case, the influence of solution flow rate was also investigated. Specifically, a series of tests (GP1) were carried out keeping the same operating conditions as those employed for Margi cases, while another set of tests was performed at higher flow rate (GP2) for both saturation (2.5 PV/h) and elution (0.8 PV/h).

Table 3 *Boron removal tests from real bitterns for two different brines (Margi(M) and Galia (G)) using two different chelating resins (Purolite S108(P) and Diaion CRB05(D))*

	MP1	MD1	GP1	GP2
Resin type	Purolite S108	Diaion CRB05	Purolite S108	Purolite S108
Bittern	Margi	Margi	Galia	Galia
Saturation flow rate	2 PV/h - 11.42 mL/min	2 PV/h - 10.7 mL/min	2 PV/h – 11.42 mL/min	2.5 PV/h - 14.66 mL/min
Regeneration flow rate	0.5 PV/h - 2.85 mL/min	0.5 PV/h – 2.67 mL/min	0.5 PV/h – 2.85 mL/min	0.8 PV/h – 4.89 mL/min

In each test, 1L of treated bittern was collected at the first PV, which was further used for $Mg(OH)_2$(s) synthesis. Other bittern samples were collected during GP2 within the first 6 PV to further investigate the influence of boron extraction on $Mg(OH)_2$(s) powder purity.

During the elution, the eluate was collected in a separate beaker from 1 PV to 1.5 PV (given that the B peak was centered at 1.5 PV) to assess boric acid recovery. However, due to the low volume collected (c.a. 150 mL), the evaporative route for boric acid crystallization was carried out with a synthetic solution mimicking the eluate composition from the MP1 and MD1. Then, an initial volume (1000 mL) was placed on a hot plate magnetic stirrer (C-MAG HS 7, IKA) to keep the solution continuously stirred at 70 °C. A sample was taken every 100 mL of evaporated water to monitor the composition change during the experiment. The test was stopped after 900 mL were evaporated, and the solution was cooled down to room temperature to promote the precipitation of salts. Then, the suspension was filtered using a 0.22 µm pore size filter and the solids collected were dried at 100ºC for 24h before analysis. The clarified was then analysed to determine the recovery of the boric acid.

2.2.2. Magnesium hydroxide precipitation

$Mg(OH)_2$(s) precipitation occurs through the reaction of magnesium and hydroxide ions:

$$Mg^{2+} + 2\ OH^- \rightarrow Mg(OH)_2(s) \quad (4)$$

A schematic representation of the $Mg(OH)_2$(s) experimental set-up is shown in Figure 4. The bittern was placed into a 1L beaker and NaOH solution was fed at a flow rate of 5 mL/min through a peristaltic pump (KRONOS 50). Bittern and, then, $Mg(OH)_2$(s) suspension were stirred at 300 rpm

by magnetic stirrer (ARGO LAB M2-A). Precipitation tests were carried out by adopting (i) a stoichiometric ratio between Mg^{2+} and OH^- amount, targeting a final suspension pH of ~10.8, and (ii) a 20 % OH^- excess. In the latter case, the final suspension pH ranged between 12 and 13. In all tests, 0.5 M NaOH solutions were employed as alkaline reactant. A final suspension volume of 800 mL was always targeted, and initial bittern and NaOH volumes were calculated consequently, taking into account also Mg^{2+} and OH^- content in the feed solutions.

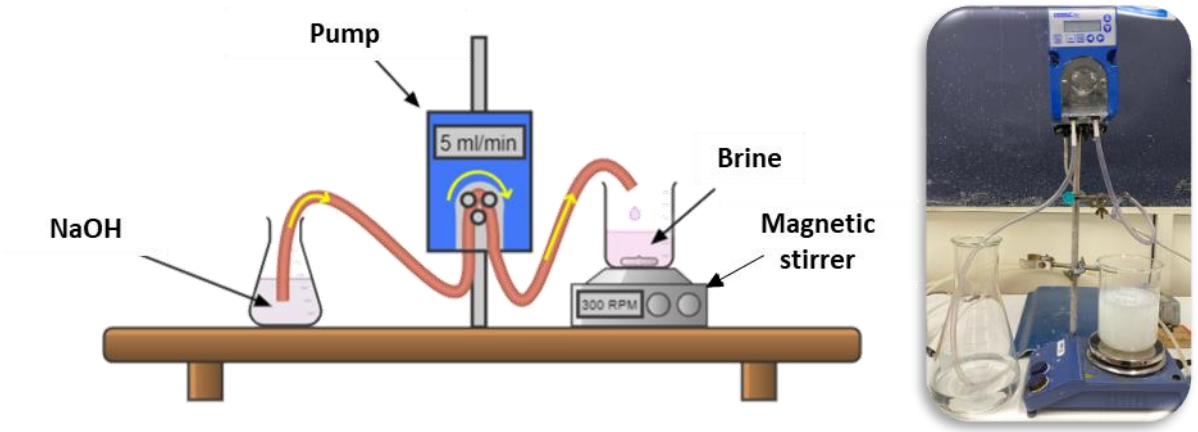

Figure 4 *Schematics of the experimental set-up for $Mg(OH)_2(s)$ precipitation tests.*

Tests were carried out using pristine bittern and the treated one, after boron removal, collected at different times (pore volumes passed in the column) during the sorption tests. All tests were performed at a room temperature. Table 4 reports the details of the $Mg(OH)_2(s)$ precipitation tests.

Table 4 *$Mg(OH)_2(s)$ precipitation tests. Tests were performed at a room temperature, using a 0.5 M NaOH solutions and by stirring bitterns and $Mg(OH)_2(s)$ suspensions at 300 rpm. Numbers from 0 to 3 refer to the PV value at which the bittern was collected (0 is the untreated bittern). The last letters S and E indicate OH^-/Mg^{2+} stoichiometric and excess amounts.*

Cases	Bittern	Bittern volume [mL]	NaOH volume [mL]	Pore Volume fraction
M_0S	**Margi (Mg^{2+} 2.04 M)**	**87.4**	**712.6**	**-**
MP1_1S	**Margi (Mg^{2+} 2.04 M)**	**87.4**	**712.6**	**1-3**
MD1_1S	**Margi (Mg^{2+} 2.04 M)**	**87.4**	**712.6**	**1-3**
M_0E	**Margi (Mg^{2+} 2.04 M)**	**69.9**	**730.1**	**-**
MP1_1E	**Margi (Mg^{2+} 2.04 M)**	**69.9**	**730.1**	**1-3**
MD1_1E	**Margi (Mg^{2+} 2.04 M)**	**69.9**	**730.1**	**1-3**
G_0S	**Galia (Mg^{2+}1.54 M)**	**111.5**	**688.5**	**-**
GP1_1S	**Galia (Mg^{2+}1.54 M)**	**111.5**	**688.5**	**1-3**
GP2_1S	**Galia (Mg^{2+}1.54 M)**	**111.5**	**688.5**	**1-2**
GP2_2S	**Galia (Mg^{2+}1.54 M)**	**111.5**	**688.5**	**3-4**
GP2_3S	**Galia (Mg^{2+}1.54 M)**	**111.5**	**688.5**	**4-6**
G_0E	**Galia (Mg^{2+}1.54 M)**	**89.2**	**710.8**	**-**
GP1_1E	**Galia (Mg^{2+}1.54 M)**	**89.2**	**710.8**	**1-3**
GP2_1E	**Galia (Mg^{2+}1.54 M)**	**89.2**	**710.8**	**1-2**
GP2_2E	**Galia (Mg^{2+}1.54 M)**	**89.2**	**710.8**	**3-4**
GP2_3E	**Galia (Mg^{2+}1.54 M)**	**89.2**	**710.8**	**5-6**

2.3. Analytical techniques

2.3.1. Analysis of liquid samples

The aqueous samples (bittern, eluate and clarified solution) were analyzed via Inductively Coupled Plasma Mass Spectrometry (ICP-MS, 7800 ICP-MS from Agilent Technologies) and Inductively Coupled Plasma Optical Emission spectroscopy (ICP-OES, Optima 2100 DV PerkinElmer spectrometer and 5100 ICP-OES from Agilent Technologies) techniques, for which samples were

previously filtered and diluted in 2% HNO_3. Samples were also analyzed using ion chromatography (IC) using, for cations, a Dionex ICS-1000 equipped with a CS16 column using 30 mM methanesulphonic acid, whereas for anions, a Dionex Aquion equipped with an IonPacTM AS11-HC column and 25 mM KOH.

2.3.2. Analysis of solid samples: $Mg(OH)_2$(s) and H_3BO_3(s)

The $Mg(OH)_2$ powder purity was assessed through three different analytical techniques: (i) X-ray diffraction, XRD; (ii) boron concentration assessment; (iii) thermogravimetric analysis, TG. X-ray analyses were conducted in the 2θ range of 10–70° (CuKa radiation 1.54°A, 40 kV, 40 mA) at a step size of 1°/min using the RIGAKU model D.MAX 2500 HK. Boron concentration in solid samples was assessed through ICP-MS, after $Mg(OH)_2$ powder acid digestion. For such purpose, 100 mg of $Mg(OH)_2$ powder were dissolved in 50 ml of 2 wt% HNO_3. TG analyses were carried out at a heating rate of 10 °C/min from 30 °C to 1000 °C, under a constant nitrogen flow of 20 mL/min using the STA 449 F1 Jupiter analyzer, NETZSCH. From TG data, the mass purity was calculated as the ratio between the mass loss recorded in the temperature range between 320 °C and 800 °C ($\Delta m_{320-800°C}$) and the theoretical one ($\Delta m_{theoretical}$, 30.87 %wt, [45]) according to eq.(5):

$$Mass\ Purity = \frac{\Delta m_{320-800°C}}{\Delta m_{theoretical}} \quad (5)$$

In the temperature range between 320 °C and 480 °C, $Mg(OH)_2$(s) decomposes into MgO(s) [45]. However, a continuous mass loss was observed between 480 °C and 800°C. Many authors have investigated this continuous loss, which has been related to the slow OH^- groups release from the MgO lattice [46–48]. Therefore, if no other impurities are identified in DTG curves (e.g. due to carbonate decomposition), namely the derivate curves of the TG ones with respect to temperature, the mass loss between 320 °C and 800 °C can be considered for $Mg(OH)_2$(s) mass purity estimation.

Boric acid samples were analysed by Field Emission Scanning Electron Microscopy Energy Dispersive X-ray Spectroscopy (FESEM-EDS) (JEOL JSM-7001F) at an acceleration voltage of 20.0 keV using Secondary Electron Imaging (SEI) or Backscattered Electrons (BE) to obtain their morphology. Apart from that, the mineral phases presented in the solid were identified with XRD, after grinding the sample into powder. A D8 Advance diffractometer (Bruker) was used with a Bragg-Brentano configuration θ-2θ and a vertical goniometer. The equipment has a Cu X-ray tube, which allows to work up to 40 kV and 40 mA. The spectrum was recorded from 15° to 60° with steps of

321 0.020°. The identification of mineral phases was performed with EVA software (Bruker). Finally,
322 samples were digested in 2% HNO_3 and then analysed by ICP to assess the solid purity.

323

3. Results and discussion

3.1. Performance of the ion-exchange resins for boron removal

3.1.1. Comparison of Purolite S108 and Diaion CRB05 for treating the Margi bittern

Boron, lithium, cobalt, gallium, germanium, rubidium, strontium and cesium breakthrough (C/C_0) and elution (using 1 M HCl) curves as a function of the volume treated by the column for the Margi bittern, expressed as PVs, are reported in Figure 5 for tests MP1 and MD1. Data for major ions is not shown, as they were not retained by the resin (C/C_0=1).

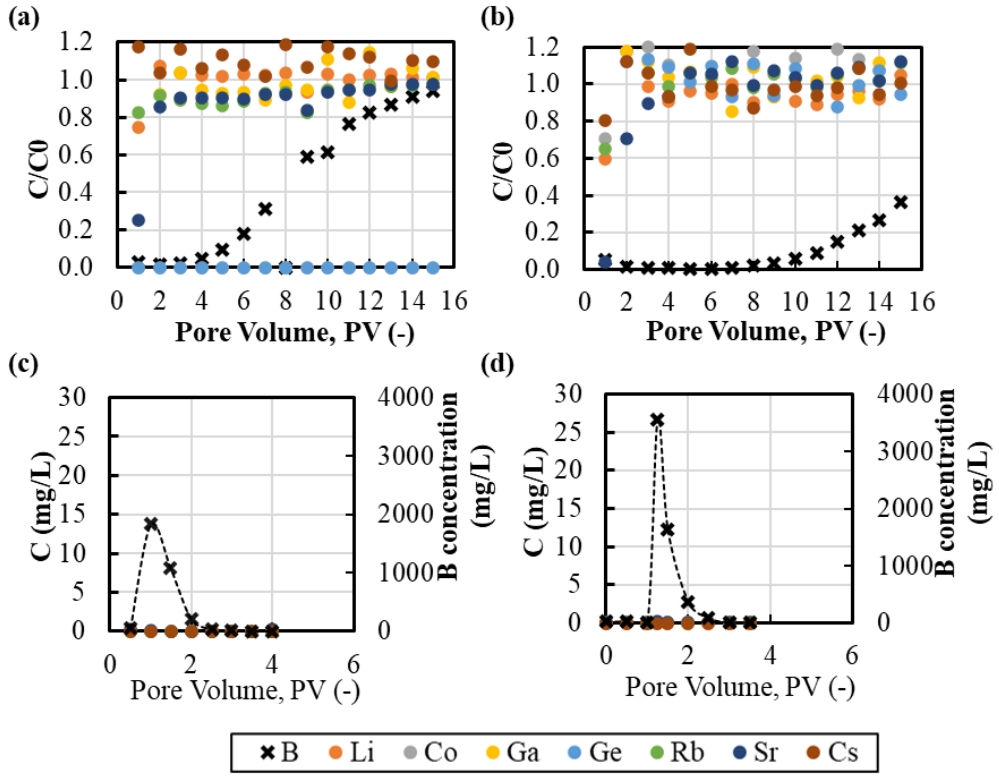

Figure 5 *(a,b) Breakthrough and (c,d) Elution curves for the trace elements (B, Li, Co, Ga, Ge, Rb, Sr and Cs) as function of pore volume for: (a,c) MP1 and (b,d) MD1*

Figure 5.a shows the performance of the Purolite S108 when treating the Margi bittern at 2 PV/h. In this case, the breakthrough of boron started around 5 PV (C/C_0 = 0.1), being the resin completely saturated on it at 16 PV. Moreover, the resin was able to extract completely the germanium in solution along the whole test. The Diaion CRB05 showed significant different performance, see Figure 5.b. As matter of fact, it can be noticed the higher capacity of the CRB05 resin, as the breakthrough for

boron started at 11 PV (C/C_0=0.1), versus the 5 PV of the S108. Moreover, in this case, germanium was note retained.

From a generic perspective, it can be observed that the two resins presented a similar behavior, confirming the high selectivity of the N-methylglucamine resins towards boron (see Figure 5.a and 5.b). It must be noted that germanium was also co-extracted by the Purolite resin, thanks to the similar chemistry of Ge and B in aqueous solutions, both forming an uncharged species (i.e. H_4GeO_4(aq) and H_4BO_4(aq)). The Ge speciation explains why it was also extracted by the N-methylglucamine functional groups, as reported by Vallès et al. [28] with an extraction mechanism similar as that described in Figure 2 for H_3BO_3(aq). This behavior for the CRB05, not reported in batch experiments with both resins and similar brines [28], was actually reported for column experiments later on [29]. The main reason may be associated to the structure changes recently introduced in the CRB05 resin, also selective for B extraction, aiming to improve the B extraction and re-extraction performance. The modification of the nature of the N-methylglucamine functional groups and the different size of the $Ge(OH)_4$(aq) molecules compared to the $B(OH)_3$(aq) molecules could therefore explain the different extraction efficiency in column mode with respect to batch mode. Apart from that, it should be highlighted the large equilibrium times used by Vallés et al. [28] during the batch experiments (24h), which are higher than the ones used under column mode in the present work (30 min).

Following elution, in the test MS1 (see Figure 5.c), the boron concentration slowly increased reaching the maximum value of 1831 mg/L at 1 PV, eventually decreasing to 0 mg/L at 3 PV, due to the continuous replacement of boron ions by H^+. In the case of other elements, their concentration remained below 0.05 mg/L. Similarly, due to the higher capacity of the CRB05, it was possible to reach a higher peak of boron during elution, being 3557 mg/L (see Figure 5.d).

3.1.2. Performance of Purolite S108 when treating the Galia bittern

Considering that Purolite S108 allows to target both boron and germanium, apart from its lower cost (half of the price in comparison to Diaion CRB05), its performance was studied with also the Galia bittern. In this case, the effect of flow rate was investigated, working at 2 PV/h and 2.5 PV/h during saturation. Boron, lithium, cobalt, gallium, germanium, rubidium, strontium and cesium breakthrough (C/C_0) and elution (using 1 M HCl) curves as a function of the volume treated by the column for the Margi bittern, expressed as PVs, are reported in Figure 6 for tests GP1 and GP2. Data for major ions is not shown, as they were not retained by the resin (C/C_0=1).

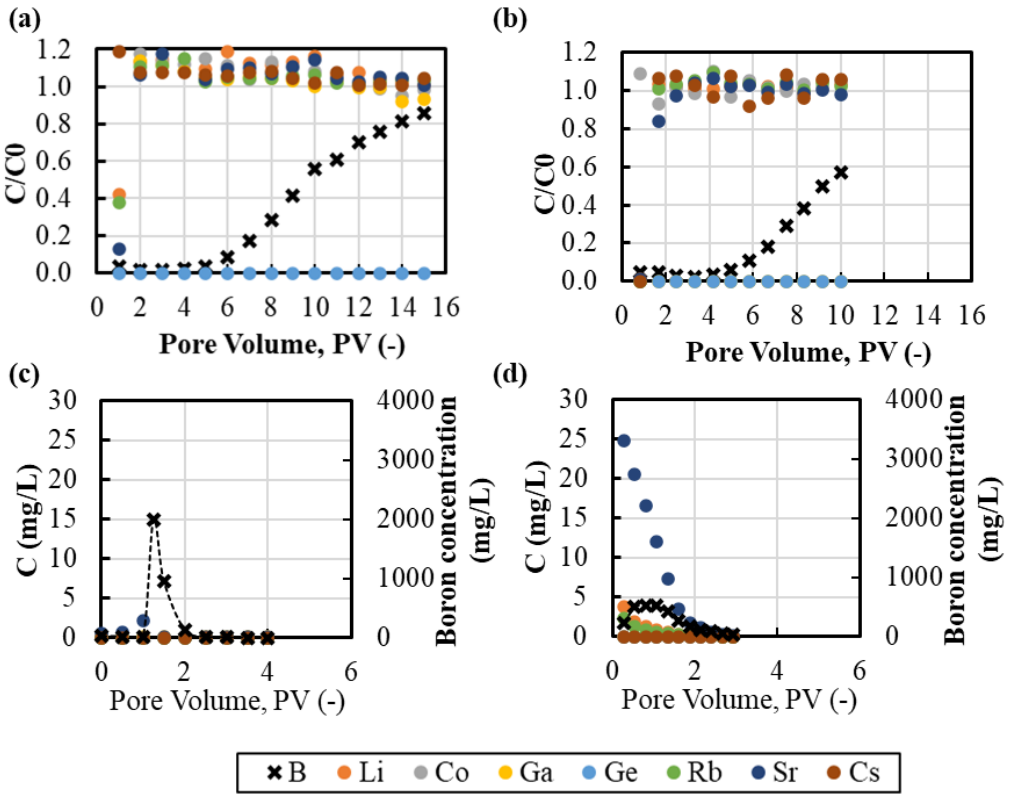

Figure 6 *(a,b) Breakthrough and (c,d) Elution curves for the trace elements (B, Li, Co, Ga, Ge, Rb, Sr and Cs) as function of pore volume for: (a,c) GP1 and (b,d) GP2.*

In the first test (Purolite S108 treating Galia bittern, with inlet flow-rate of 2 PV/h, Figure 6.a), the breakthrough for boron started at around 6 PV (C/C_0=0.1), while Ge was completely extracted G(C/C_0=0) during the whole test (10 PV). In comparison to the previous test (MP1), the breakthrough started later, likely due to a slightly lower boron concentration (133 mg/L vs 161 mg/L). Ge sorption was quantitative as in the other test with Purolite resin. When the flow rate was increased to 2.5 PV/h, during the resin saturation, already in the initial phase of the test, boron was not completely removed, as the C/C_0 was around 0.05, likely due to the high velocity inside the column.

Following saturation of the resin, elution was carried out using 1 M HCl and the concentration profiles plotted in Figure 6 were found, as a function of the volume of HCl used (converted to PVs). In the test GP1, where elution was performed at 0.5 PV/h, the resin presented a similar trend as the MP1 test, reaching a boron peak of 2000 mg/L at 1.25 PV. However, during the elution at 0.8 PV/h, the boron concentration slowly increased reaching the maximum value of 500 mg/L at 1 PV, eventually decreasing to 0 mg/L at 3 PV. It should be noted that a wide peak was obtained rather than a clearly defined peak due to the higher velocity of HCl inside the column. In the case of other elements, the

strontium concentration decreased from 25 mg/L to 0 in the first 2PV. Traces of gallium, lithium and rubidium were observed in the first 2 PV (from ~4 mg/L to <0.1 mg/L). The presence of these elements in the eluate, that were not extracted by the resin, were likely related to an un-efficient bittern washing-out step between saturation and elution.

3.1.3. Comparison among scenarios: boron removal, resins capacity, concentration factor and recovery percentage

As mentioned previously, the solution after being treated by the resin was collected to be later used for $Mg(OH)_2$(s) crystallization. Figure 7 shows the boron concentrations in the initial bitterns and in the samples collected for both Galia (Figure 7.a) and Margi (Figure 7.b) bittern. The boron content was considerably reduced in samples collected at the first 3 PV regardless the treated bittern (Margi or Galia) or the adopted flow rate (GP1 and GP2 cases). With the samples collected from 1 to 3 PV, it was possible to reduce boron concentration to values lower than 17 mg/L (MD1) or below the quantification limits of ICP, namely 7.2 and 26.78 mg/L for Margi and Galia bitterns analyses. However, in the test GP2, the boron concentration increased to a value of 37.9 mg/L (GP2_3) at the sample collected from 4 to 6 PV, indicating the start of the breakthrough curve.

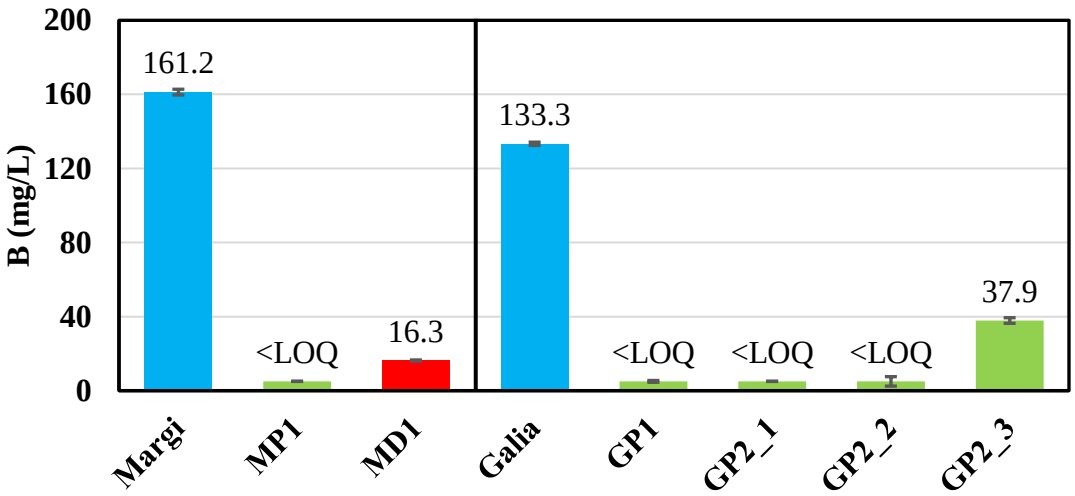

Figure 7 *Boron concentration in Margi and Galia Margi bitterns with and without the treatment using ion-exchange resins. GP1_1, 2, 3 PV refer to samples withdrawn within 0-2, 2-4 and 4-6 PV treated in the resin, while all the other samples were collected within 1 and 3 PV.*

Figure 8 shows the final boron concentration in the collected eluate. In this case, in order to maximize boron concentration, the eluate was collected from 1 to 1.5 PV, which is the region where the peak was centered. As expected, the lowest concentration was in the GP2 due to the higher flow rate during elution, while decreasing elution flow-rate to 0.5 PV/h, higher concentration values were obtained ranging from 1.3 g/L for the S108 resin up to 1.9 g/L for the CRB05. The higher concentration factors achieved in test MD1 reflects the improvements done in CRB05 to optimize its extraction-re-extraction systems.

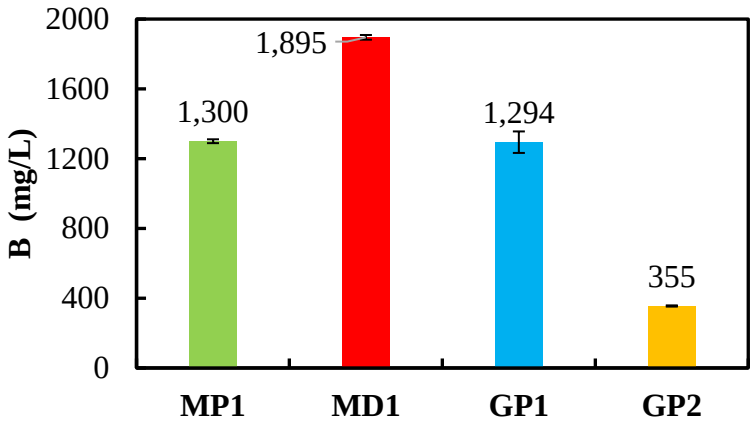

Figure 8 *Boron concentration in the eluate solutions collected from 1 to 1.5 PV for the four B recovery/removal tests performed.*

From the analysis of results presented, the main process performance indicators were calculated, namely resin capacity, B concentration factor and B-recovery, and are reported in Table 5 for all tests.

Table 5 *Resin capacity, B concentration factor and B-recovery*

	Resin capacity (mg/g)	**Concentration factor (CF)**	**% B recovery**
MD1	1.6	11.8	>99.9
MP1		8.1	>99.9
GP1	1.2±0.1	9.7	96.8
GP2		2.7	97.6

The Purolite S108 resin exhibited a capacity of ~1.2 (±0.1) mg B/g, which was consistent along the different tests performed (tests MP1, GP1 and GP2). The Diaion CRB05 exhibited the highest resin

426 capacity, with a value of 1.6 mg/g (MD1). In terms of concentration factor, it was also observed the
427 effect of decreasing the flow-rate during elution, as it was possible to increase it from 2.7 to 9.7 (test
428 GP2 to test GP1). By comparing the performance of the two resins, it was also noticed that the CRB05
429 allowed to achieve higher CF values (11.8) in front of S108 (8.1) under the same operating conditions.
430 With regard to the efficacy of the regeneration process, more than 97% of the boron extracted was
431 later recovered in the elution for all tests.

432 The capacities obtained were lower than the ones from the literature. For instance, Figueira et al. [26]
433 reported an adsorption capacity around 13 mg/g for CRB03 (differences with CRB05 are related to
434 the porous support) after testing it in column mode. Apart from that, Vallès et al. [29] obtained
435 adsorption capacity values from 3.8 to 9.0 mg B/g for S108 and from 9.1 to 12 mg B/g resin for
436 CRB05. It should be mentioned that the discrepancies between the values arise due to the fact that
437 the ones present in **Table 4** were determined using the data till the breakthrough point ($C/C_0 = 0.1$),
438 whereas the data from the literature was reported after reaching a complete saturation of the resin.
439 With regard to the concentration factor, Vallès et al. [29] reported the possibility to concentrate boron
440 up to 7.4 for S108 and up to 9.6 for CRB05, which are in agreement with the data here obtained.
441 Finally, with respect to the desorption efficiency, similar values were achieved as Jung and Kim [49]
442 and Vallès et al. [29].

443

444 ### 3.1.4. Boron recovery from the eluate

445 A synthetic solution mimicking the eluate from MP1 and GP1 3 was used to crystallize B via an
446 evaporative route, as reported by Vallès et al. [35].

447 Figure 9 shows the concentration profiles as function of the water evaporated (in %). It can be
448 observed that the concentration of different elements tended to increase as water was evaporated until
449 reaching a value of 90%. Once this point was reached, the solution was cooled down, which caused
450 the precipitation of boron, evident in the figure by the B concentration decrease from 13.2 g/L to 4.1
451 g/L. It should be highlighted that the other elements in solution did not precipitate.

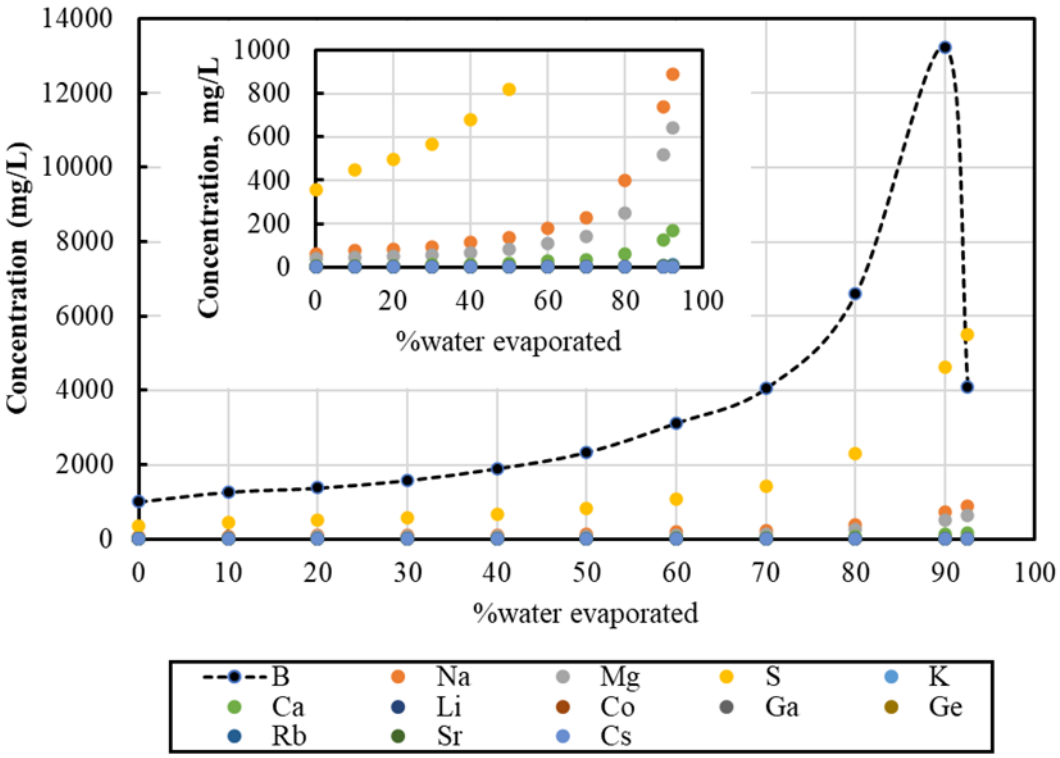

Figure 9 *Boron and other Trace Elements concentration in the eluate solutions during the evaporation/concentration step. The inset shows a zoom in the low-concentration range for the trace elements.*

The solids collected were analyzed by FESEM-EDAX (Fig. 10), showing small (<10 μm), flat and uniform crystals. When the solids were analyzed by EDAX, only the presence of B was noticed. It should be noted that the presence of oxygen by EDAX might be related to the H_3BO_3(s), but also to the polymeric support used.

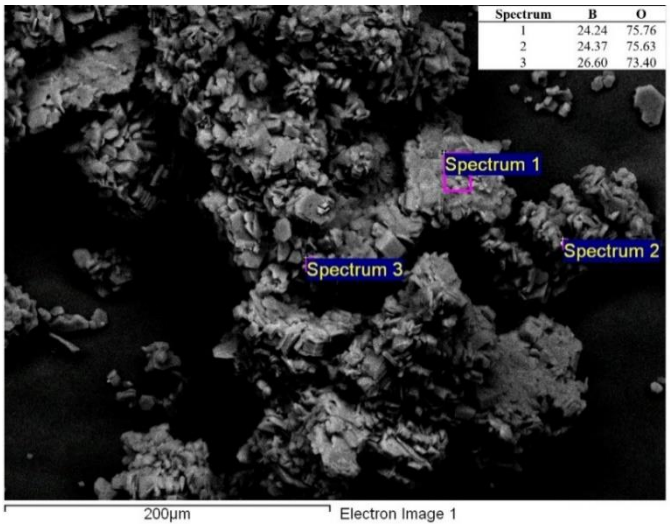

462

463 ***Figure 10*** *FESEM-EDAX analysis, showing crystals morphology and elemental composition of the*
464 *solid (B and O can be related to the boric acid nature of crystals)*

465

466 When acid digestion was performed, followed by ICP analysis, the solid revealed a high content of
467 B, which was equal to 973.2±5.9 mg H_3BO_3/g, see Table 6. With regard to the impurities within the
468 solid, it was observed that they were mostly related to S and Sr, which could be related to any likely
469 precipitation of $SrSO_4$(s). other elements remained below 0.6% (Table 6).

470

471 ***Table 6*** *Composition of the solids following acid digestion 2% HNO_3 and analysis by ICP. No traces*
472 *of Li, Ga, Rb and Cs were detected.*

Element	mg/g	%
B	170.2±1.1	95.6±2.5
Ca	0.36±0.11	0.20±0.05
Mg	0.18±0.09	0.10±0.05
Na	0.99±0.39	0.55±0.20
S	1.57±0.98	0.88±0.52
K	0.16±0.04	0.09±0.02
Co	0.99±0.24	0.55±0.12
Ge	0.73±0.33	0.40±0.17
Sr	2.91±1.74	1.62±0.93

3.2. Analysis of precipitated $Mg(OH)_2$(s) samples

3.2.1. Boron content in $Mg(OH)_2$(s) samples

The major focus of precipitation experiments from the B-treated bitterns was to identify whether the B presence in the precipitated $Mg(OH)_2$(s) could be effectively reduced by the proposed pre-treatment. With this respect, the boron content in synthesized $Mg(OH)_2$ powders was measured by ICP-MS technique for all precipitation experiments performed and results are reported in **Figure 11**.

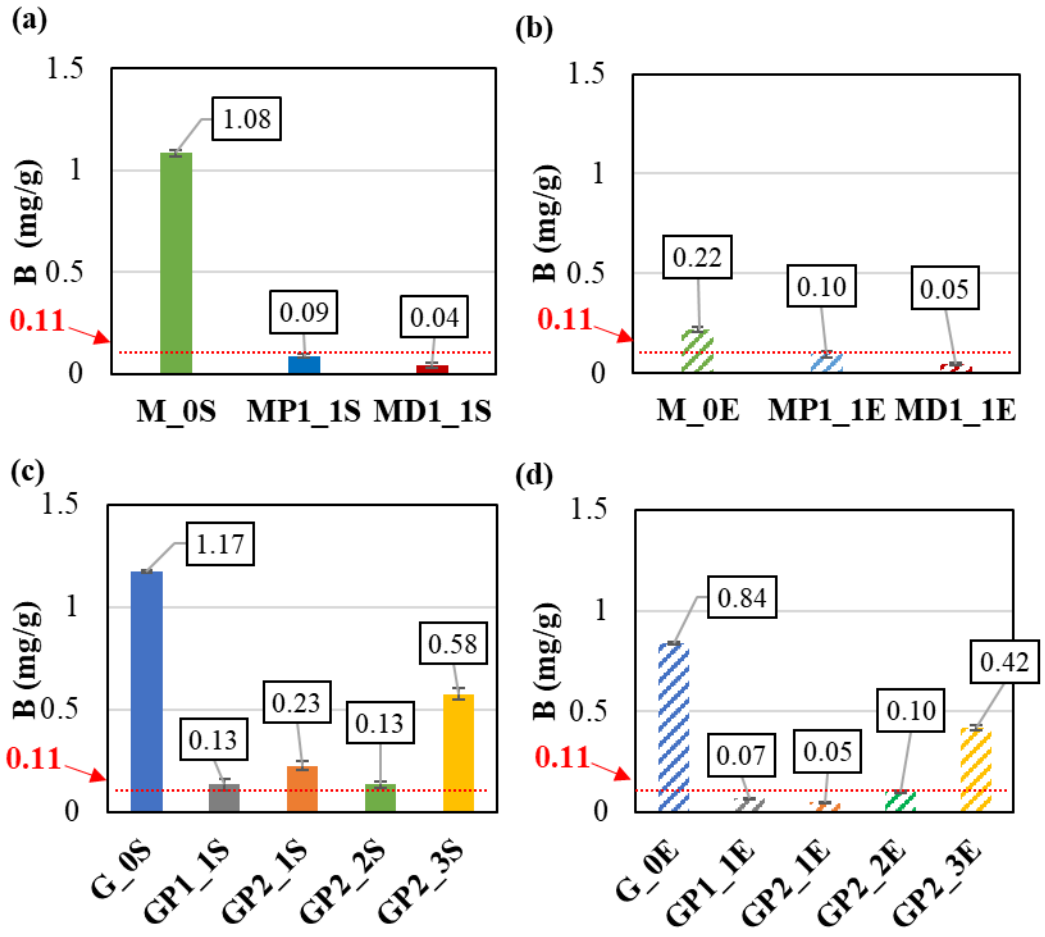

Figure 11 *Boron concentration in $Mg(OH)_2$(s) samples precipitated from virgin and treated (boron-free) bitterns. Experimental conditions for each tests are reported in* ***Table 4****. The red dotted line indicates the boron threshold concentration of ~0.11 mg B/g for the refractory industry [39].*

Boron content ranged between 1.2 and 1.1 mg B/g in $Mg(OH)_2$(s) samples synthesized from un-treated Margi and Galia bitterns by adopting OH^-/Mg^{2+} stoichiometric amounts, namely M_0S and G_0S samples (Figure 11 a and c), while it was almost one order of magnitude lower, i.e. ~0.1-0.2

mg B/g, in samples produced from bitterns collected at the first 4 PVs (Figure 11 a and c). It can be observed, in fact, that the boron content in the sample GP2_3S, which was synthesized by using the bittern collected at 4-6 PVs, increased in accordance with the boron content measured in the treated bitterns. $Mg(OH)_2$ powders synthesized by adopting OH^-/Mg^{2+} excess amounts exhibited lower boron contents. This was somehow expected [50]. The pH of the reaction environment, in fact, strongly influences the boron adsorption on $Mg(OH)_2$(s) surfaces. The boron adsorption mechanism has been described to occur between OH^- groups of $Mg(OH)_2$(s) compounds and $B(OH)_4^-$ ions [51]. $Mg(OH)_2$ particles are characterized by a positive and negative electric charge below and above pH 12 (isoelectric point) [52]. The different charge of the particles favors or hinders the interaction with $B(OH)_4^-$ ions. Below the isoelectric point, $B(OH)_4^-$ ions are adsorbed onto $Mg(OH)_2$ particles, while above the isoelectric point, $B(OH)_4^-$ ions are mostly rejected. The highest boron concentrations were ~0.84, ~0.42 and ~0.22 mg B/g in G_0E, GP2_3E and M_0E samples, respectively, see Figure 11 b and d. Conversely, the pH environment did not significantly affect the boron content in $Mg(OH)_2$(s) samples produced from treated bitterns collected at the first 0-3 PVs that was always lower than ~0.10 mg B/g. In these samples, boron content was almost the same as that observed in samples synthesized under stoichiometric reagents conditions. This result confirms the effective boron removal by the resins.

As discussed in the introduction section, the boron content in $Mg(OH)_2$ powders can limit their applicability in several industrial sectors. As an example, in the refractory industry, the boron concentration must be lower than a threshold value of ~0.11 mg B/g [39]. As can be seen in Figure 11, powders synthesised from treated bitterns collected in the first 1-4 PVs reported boron concentrations lower or slightly above, i.e. 13 mg B/g against 11 mg B/g, the threshold one. This threshold value was always considerably exceeded, when adopting untreated bitterns even using OH^-/Mg^{2+} excess amounts, thus making the resin adsorption pre-treatment in all cases a reliable step for boron removal and $Mg(OH)_2$ particles production for refractory applications.

3.2.2. $Mg(OH)_2$(s) purity determination by TG analysis

Boron content in $Mg(OH)_2$ powders is expected to affect their mass purity. $Mg(OH)_2$(s) mass purity values measured via TG analysis for samples synthesized from treated and untreated bitterns are reported in Figure 12.

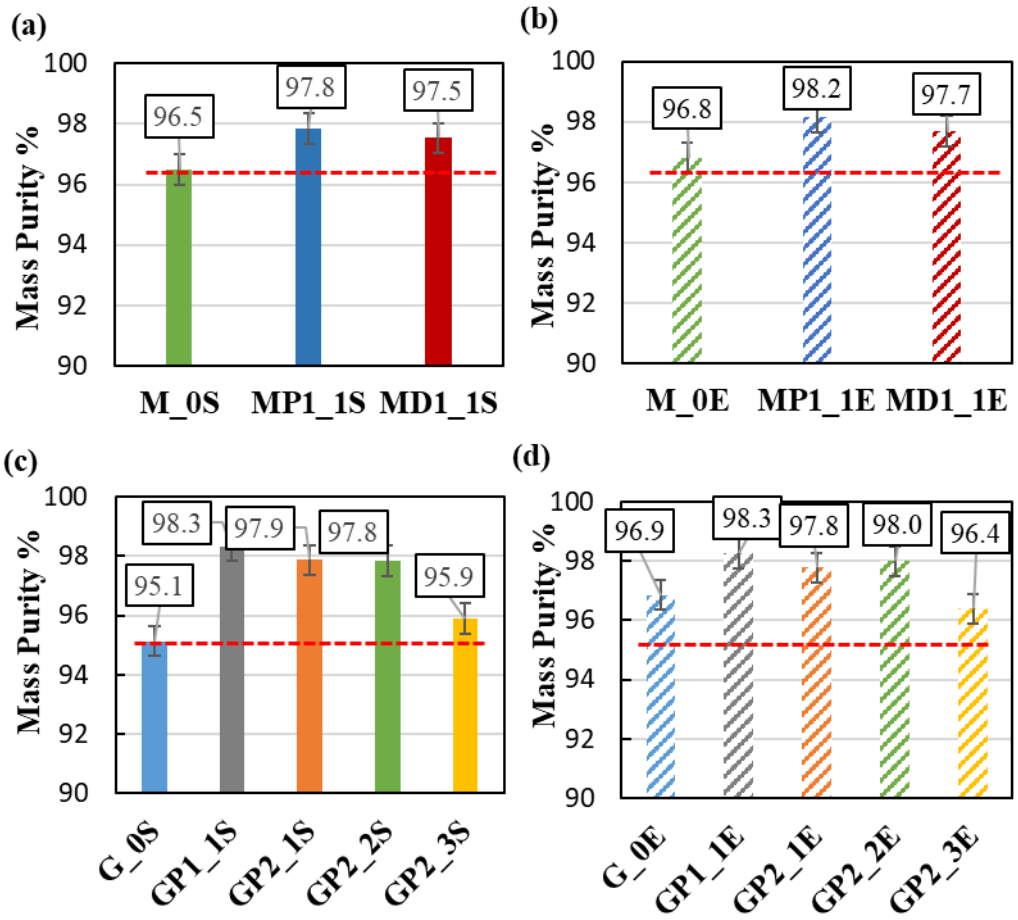

517

518 ***Figure 12*** *$Mg(OH)_{2(s)}$ purity values determined by TG of samples synthesized from treated and*
519 *untreated bitterns. Red dashed line is the mass purity value evaluated for cases M_0S and G_0S.*

520

521 The mass purity trend very well agreed with the boron content reduction in solids. The lowest mass
522 purity values were measured in samples synthesized from the untreated bitterns under OH^-/Mg^{2+}
523 stoichiometric conditions, namely 96.5% and 95.1% in M_0S and G_0S samples, respectively. Mass
524 purity increased in powders synthesized from virgin bitterns by adopting an OH^-/Mg^{2+} amount excess
525 reaching values of ~96.8% in both M_0E and G_0E samples. $Mg(OH)_2$ solids produced from bitterns
526 collected between the first 0-4 PVs showed mass purities always higher than 97.5 % under OH^-/Mg^{2+}
527 stoichiometric and OH^- amount excess. One again, mass purity of samples GP2_1S, GP2_2S and
528 GP2_3S followed the boron content evidence of **Figure 11**. Specifically, mass purity decreased in
529 sample GP2_3S due to the saturation of the resin.
530 Unfortunately, it is difficult to predict the possible mass purity percentage attributed to boron
531 compounds. H_3BO_3 and $B(OH)_4^-$ species, in fact, are expected to interact with $Mg(OH)_2(s)$
532 compounds to form more stable multi-coordination compounds [53]. Due to the special coordination

property of boron, many kinds of boron oxygen coordination anions in boron aqueous solution (such as $[B_3O_3(OH)_{4)}]^{2-}$, $[B_4O_5(OH)_4)]^{2-}$) can be formed leading to the uncertainty of the formation of different boron magnesium compounds [53].

3.2.3. Mineralogical characterization of $Mg(OH)_2$(s) samples by XRD

The possible boron presence in synthesized $Mg(OH)_2$ powders was also investigated through XRD analyses. Figure 13 shows the XRD pattern of the $Mg(OH)_2$ powder synthesized in the M_0S test.

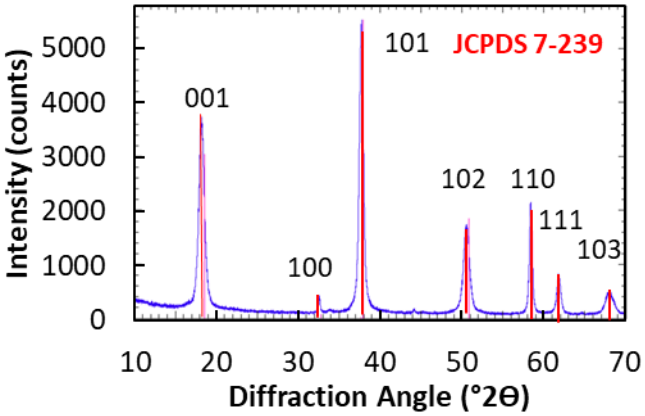

Figure 13 *XRD pattern of the $Mg(OH)_2$ powder synthesized in the M_0S test. Characteristic peaks of magnesium hydroxide (brucite) mineral are highlighted in red (JCPDS 7-239).*

Only characteristic peaks of the brucite mineral are identified in the XRD pattern. This can be attributed to the low boron content that could not be detected by the adopted technique. Similar patterns were identified in all other cases, here omitted for the sake of brevity.

4. Conclusions

In this study, the integration of ion-exchange technology and crystallization was evaluated to recover boric acid and magnesium hydroxide from *bitterns.* The results indicated the possibility to recover pure magnesium hydroxide (>98%) with a low content of boron (<~0.11 mg B/g), which can make possible to use it in the refractory industry.

Initially, the performance of N-methylglucamine based resins was evaluated to treat two different bitterns, differing on initial concentrations. It was observed that both resins evaluated (S108 and CRB05) effectively removed boron, being the CRB05 the one that showed a best performance in terms of capacity and concentration factor achieved. However, it should be noted that Purolite S108 was the only one that was able to target both boron and germanium. It should be also highlighted the fact that resins were effectively regenerated using 1 M HCl. Following elution, it was possible to recover the boron via an evaporative crystallization as boric acid, resulting on a purity of 95.61±2.45%.

In the case of magnesium crystallization, it was observed that the solids presented between 1.2 and 1.1 mg B/g if the bittern is treated as it is. However, the solids presented concentrations below 0.1 mg B/g by pre-treating the resins with ion-exchange resins. Apart from that, the integration of ion-exchange resins resulted in an increase of the magnesium hydroxide purity from 95.1% (no pre-treatment) to ~98 %.

Acknowledgments

This project has received funding from the European Union's Horizon 2020 research and innovation programme under Grant Agreement No. 869467 (SEArcularMINE). This output reflects only the author's view. The European Health and Digital Executive Agency (HaDEA) and the European Commission cannot be held responsible for any use that may be made of the information contained therein. J. López research was developed under the Margarita Salas postdoctoral fellowship from Ministerio de Universidades (MIU) and funded by the European Union-NextGeneration EU. Support for the research of J.L. Cortina was also received through the "ICREA Academia" recognition for excellence in research funded by the Generalitat de Catalunya. Authors acknowledge the support of R. Cucchiara during the experimental campaign.

Author Statement

Julio López, Conceptualization, Methodology, Validation, Formal analysis, Investigation, Data Curation, Writing - Original Draft, Visualization, Supervision.

Giuseppe Battaglia, Conceptualization, Methodology, Validation, Formal analysis, Investigation, Data Curation, Writing - Original Draft, Visualization, Supervision.

Dario Lupo, Validation, Formal analysis, Investigation, Data Curation, Visualization.

Marc Fernández de Labastida, Methodology, Validation, Formal analysis, Investigation, Data Curation.

Víctor Vallès, Methodology, Validation, Formal analysis, Investigation, Data Curation, Writing - Original Draft, Visualization.

Jose Luis Cortina, Conceptualization, Methodology, Resources, Writing - Review & Editing, Supervision, Project administration, Funding acquisition.

Andrea Cipollina, Conceptualization, Methodology, Resources, Writing - Review & Editing, Supervision, Project administration, Funding acquisition.

Giorgio Micale, Conceptualization, Methodology, Resources, Supervision, Project administration, Funding acquisition.

References

[1] European Commission, Critical raw materials | Internal Market, Industry, Entrepreneurship and SMEs, (2023).

[2] European Commission, M. Grohol, C. Veeh, Study on the critical raw materials for the EU 2023 – Final report, 2023. https://doi.org/10.2873/725585.

[3] A. Kumar, G. Naidu, H. Fukuda, F. Du, S. Vigneswaran, E. Drioli, J.H. Lienhard, Metals Recovery from Seawater Desalination Brines: Technologies, Opportunities, and Challenges, ACS Sustain. Chem. Eng. 9 (2021) 7704–7712. https://doi.org/10.1021/acssuschemeng.1c00785.

[4] C.A. Quist-Jensen, F. Macedonio, E. Drioli, Membrane crystallization for salts recovery from

603 brine—an experimental and theoretical analysis, Desalin. Water Treat. 57 (2016) 7593–7603.
604 https://doi.org/10.1080/19443994.2015.1030110.

605 [5] X. Zhang, W. Zhao, Y. Zhang, V. Jegatheesan, A review of resource recovery from seawater
606 desalination brine, Rev. Environ. Sci. Biotechnol. 20 (2021) 333–361.
607 https://doi.org/10.1007/s11157-021-09570-4.

608 [6] T. Jeppesen, L. Shu, G. Keir, V. Jegatheesan, Metal recovery from reverse osmosis concentrate,
609 J. Clean. Prod. 17 (2009) 703–707. https://doi.org/10.1016/j.jclepro.2008.11.013.

610 [7] U. Bardi, Extracting minerals from seawater: An energy analysis, Sustainability. 2 (2010) 980–
611 992. https://doi.org/10.3390/su2040980.

612 [8] A. Shahmansouri, J. Min, L. Jin, C. Bellona, Feasibility of extracting valuable minerals from
613 desalination concentrate: A comprehensive literature review, J. Clean. Prod. 100 (2015) 4–16.
614 https://doi.org/10.1016/j.jclepro.2015.03.031.

615 [9] P. Loganathan, G. Naidu, S. Vigneswaran, Mining valuable minerals from seawater: A critical
616 review, Environ. Sci. Water Res. Technol. 3 (2017) 37–53.
617 https://doi.org/10.1039/c6ew00268d.

618 [10] B.K. Pramanik, L.D. Nghiem, F.I. Hai, Extraction of strategically important elements from
619 brines: Constraints and opportunities, Water Res. 168 (2020).
620 https://doi.org/10.1016/j.watres.2019.115149.

621 [11] SEArcularMINE, (n.d.). https://searcularmine.eu (accessed March 1, 2022).

622 [12] J.S. Davis, Structure, function and management of the biological system for seasonal solar
623 saltworks, Glob. NEST J. 2 (2018) 217–226. https://doi.org/10.30955/gnj.000175.

624 [13] S. Gorjian, F.J. Jamshidian, B. Hosseinqolilou, Feasible Solar Applications for Brines Disposal
625 in Desalination Plants, in: A. Kumar, O. Prakash (Eds.), Sol. Desalin. Technol., Springer,
626 Singapore, 2019: pp. 25–48. https://doi.org/10.1007/978-981-13-6887-5.

627 [14] F. Vicari, S. Randazzo, J. López, M.F. de Labastida, V. Vallès, G. Micale, A. Tamburini, G.D.
628 Staiti, J.L. Cortina, A. Cipollina, M. Fernández de Labastida, V. Vallès, G. Micale, A.
629 Tamburini, G. D'Alì Staiti, J.L. Cortina, A. Cipollina, Mining minerals and critical raw
630 materials from bittern: Understanding metal ions fate in saltwork ponds, Sci. Total Environ.
631 847 (2022). https://doi.org/10.1016/j.scitotenv.2022.157544.

632 [15] S. Randazzo, F. Vicari, J. López, M. Salem, R. Lo Brutto, S. Azzouz, S. Chamam, S. Cataldo,

N. Muratore, M. Fernández de Labastida, V. Vallès, A. Pettignano, G. D'Alì Staiti, S. Pawlowski, A. Hannachi, J.L. Cortina, A. Cipollina, Unlocking hidden mineral resources: Characterization and potential of bitterns as alternative sources of critical raw materials, J. Clean. Prod. 436 (2024) 140412. https://doi.org/10.1016/j.jclepro.2023.140412.

[16] European Commission, Study on the EU's list of Critical Raw Materials (2020) Final Report, 2020. https://doi.org/10.2873/11619.

[17] M.-O. Simonnot, C. Castel, M. Nicolaï, C. Rosin, M. Sardin, H. Jauffret, Boron removal from drinking water with a boron selective resin: Is the treatment really selective?, Water Res. 34 (2000) 109–116. https://doi.org/10.1016/S0043-1354(99)00130-X.

[18] M.M. Nasef, M. Nallappan, Z. Ujang, Polymer-based chelating adsorbents for the selective removal of boron from water and wastewater: A review, React. Funct. Polym. 85 (2014) 54–68. https://doi.org/10.1016/j.reactfunctpolym.2014.10.007.

[19] J. Wolska, M. Bryjak, Methods for boron removal from aqueous solutions — A review, Desalination. 310 (2013) 18–24. https://doi.org/10.1016/j.desal.2012.08.003.

[20] Z. Guan, J. Lv, P. Bai, X. Guo, Boron removal from aqueous solutions by adsorption - A review, Desalination. 383 (2016) 29–37. https://doi.org/10.1016/j.desal.2015.12.026.

[21] N. Kabay, S. Sarp, M. Yuksel, Ö. Arar, M. Bryjak, Removal of boron from seawater by selective ion exchange resins, React. Funct. Polym. 67 (2007) 1643–1650. https://doi.org/10.1016/j.reactfunctpolym.2007.07.033.

[22] N. Kabay, E. Güler, M. Bryjak, Boron in seawater and methods for its separation - A review, Desalination. 261 (2010) 212–217. https://doi.org/10.1016/j.desal.2010.05.033.

[23] E. Çermikli, F. Şen, E. Altıok, J. Wolska, P. Cyganowski, N. Kabay, M. Bryjak, M. Arda, M. Yüksel, Performances of novel chelating ion exchange resins for boron and arsenic removal from saline geothermal water using adsorption-membrane filtration hybrid process, Desalination. 491 (2020) 114504. https://doi.org/10.1016/j.desal.2020.114504.

[24] L. Melnyk, V. Goncharuk, I. Butnyk, E. Tsapiuk, Boron removal from natural and wastewaters using combined sorption/membrane process, Desalination. 185 (2005) 147–157. https://doi.org/10.1016/j.desal.2005.02.076.

[25] S. Nishihama, Y. Sumiyoshi, T. Ookubo, K. Yoshizuka, Adsorption of boron using glucamine-based chelate adsorbents, Desalination. 310 (2013) 81–86.

https://doi.org/10.1016/j.desal.2012.06.021.

[26] M. Figueira, M. Reig, M. Fernández de Labastida, J.L. Cortina, C. Valderrama, Boron recovery from desalination seawater brines by selective ion exchange resins, J. Environ. Manage. 314 (2022). https://doi.org/10.1016/j.jenvman.2022.114984.

[27] Z. Hubicki, D. Koodynsk, Selective Removal of Heavy Metal Ions from Waters and Waste Waters Using Ion Exchange Methods, in: Ion Exch. Technol., InTech, 2012. https://doi.org/10.5772/51040.

[28] V. Vallès, J. López, M. Fernández de Labastida, O. Gibert, A. Leskinen, R.T. Koivula, J.L. Cortina, Polymeric and inorganic sorbents as a green option to recover critical raw materials at trace levels from sea saltwork bitterns, Green Chem. (2023). https://doi.org/10.1039/D2GC02338E.

[29] V. Vallès, M.F. de Labastida, J. López, J.L. Cortina, Selective recovery of boron, cobalt, gallium and germanium from seawater solar saltworks brines using N-methylglucamine sorbents: Column operation performance, Sci. Total Environ. 923 (2024) 171438. https://doi.org/10.1016/j.scitotenv.2024.171438.

[30] J.Y. Lin, N.N.N. Mahasti, Y.H. Huang, Recent advances in adsorption and coagulation for boron removal from wastewater: A comprehensive review, J. Hazard. Mater. 407 (2021) 124401. https://doi.org/10.1016/j.jhazmat.2020.124401.

[31] D. Chorghe, M.A. Sari, S. Chellam, Boron removal from hydraulic fracturing wastewater by aluminum and iron coagulation: Mechanisms and limitations, Water Res. 126 (2017) 481–487. https://doi.org/10.1016/j.watres.2017.09.057.

[32] H.C. Tsai, S.L. Lo, Boron recovery from high boron containing wastewater using modified sub-micron Ca(OH)2 particle, Int. J. Environ. Sci. Technol. 12 (2015) 161–172. https://doi.org/10.1007/s13762-013-0413-y.

[33] R. Vaghetto, M. Childs, P. Jones, S. Lee, E. Kee, Y.A. Hassan, Experimental observations of boric acid precipitation scenarios, Nucl. Eng. Des. 312 (2017) 422–428. https://doi.org/10.1016/j.nucengdes.2016.04.045.

[34] R. He, T. Yu, J. Du, C. Qu, Study on the Existence Form and Removal of Boron Acid, in: IOP Conf. Ser. Mater. Sci. Eng., 2019: p. 012059. https://doi.org/10.1088/1757-899X/484/1/012059.

693 [35] V. Vallès, M. de Labastida, J. López, G. Battaglia, D. Winter, S. Randazzo, A. Cipollina, J.L.
694 Cortina, Sustainable recovery of critical elements from seawater saltworks bitterns by
695 integration of high selective sorbents and reactive precipitation and crystallisation: Developing
696 the probe of concept with on-site produced chemicals and energy, Sep. Purif. Technol. 306
697 (2023). https://doi.org/10.1016/j.seppur.2022.122622.

698 [36] S. Romano, S. Trespi, R. Achermann, G. Battaglia, A. Raponi, D. Marchisio, M. Mazzotti, G.
699 Micale, A. Cipollina, The Role of Operating Conditions in the Precipitation of Magnesium
700 Hydroxide Hexagonal Platelets Using NaOH Solutions, Cryst. Growth Des. 23 (2023) 6491–
701 6505. https://doi.org/10.1021/acs.cgd.3c00462.

702 [37] A.A. Pilarska, Ł. Klapiszewski, T. Jesionowski, Recent development in the synthesis,
703 modification and application of Mg(OH)2 and MgO: A review, Powder Technol. 319 (2017)
704 373–407. https://doi.org/10.1016/j.powtec.2017.07.009.

705 [38] Housh et al., Method of Producing Magnesium, US4229423A, 1980.

706 [39] Spoors et al., MANUFACTURE OF MAGNESIUM, 4,497,781, 1985.

707 [40] Wilkomirsky, PROCESS FOR EXTRACTING THE BORON CONTENT IN THE BRINE OF
708 NATURAL OR INDUSTRIAL SALT MINES, US005676916A, 1997.

709 [41] F.Q. Li, B.P. Ling, P.H. Ma, Manufacture of boron-free magnesia with high purity from residual
710 brine, Chinese Chem. Lett. 15 (2004) 1353–1356.

711 [42] L. Bonin, D. Deduytsche, M. Wolthers, V. Flexer, K. Rabaey, Boron extraction using selective
712 ion exchange resins enables effective magnesium recovery from lithium rich brines with
713 minimal lithium loss, Sep. Purif. Technol. 275 (2021).
714 https://doi.org/10.1016/j.seppur.2021.119177.

715 [43] Purolite S108 Product Data Sheet, (n.d.).

716 [44] Diaion CRB05 Product Data Sheet, (n.d.).

717 [45] A. Sierra-Fernandez, L.S. Gomez-Villalba, O. Milosevic, R. Fort, M.E. Rabanal, Synthesis and
718 morpho-structural characterization of nanostructured magnesium hydroxide obtained by a
719 hydrothermal method, Ceram. Int. 40 (2014) 12285–12292.
720 https://doi.org/10.1016/j.ceramint.2014.04.073.

721 [46] S. Ardizzone, C.L. Bianchi, M. Fadoni, B. Vercelli, Magnesium salts and oxide: An XPS
722 overview, Appl. Surf. Sci. 119 (1997) 253–259. https://doi.org/10.1016/S0169-

4332(97)00180-3.

[47] G. Battaglia, M.A. Domina, R. Lo Brutto, J. Lopez Rodriguez, M. Fernandez de Labastida, J.L. Cortina, A. Pettignano, A. Cipollina, A. Tamburini, G. Micale, Evaluation of the Purity of Magnesium Hydroxide Recovered from Saltwork Bitterns, Water (Switzerland). 15 (2023). https://doi.org/10.3390/w15010029.

[48] D. Zhang, P. Zhang, S. Song, Q. Yuan, P. Yang, X. Ren, Simulation of magnesium hydroxide surface and interface, J. Alloys Compd. 612 (2014) 315–322. https://doi.org/10.1016/j.jallcom.2014.05.198.

[49] S. Jung, M.J. Kim, Optimal conditions for recovering boron from seawater using boron selective resins, Korean J. Chem. Eng. 33 (2016) 2411–2417. https://doi.org/10.1007/s11814-016-0096-4.

[50] M.A. Shand, The chemistry and technology of magnesia, Wiley-Interscience, 2006.

[51] M. Del Mar De La Fuente Garcia-Soto, E.M. Camacho, Boron removal by means of adsorption with magnesium oxide, Sep. Purif. Technol. 48 (2006) 36–44. https://doi.org/10.1016/j.seppur.2005.07.023.

[52] G. Battaglia, S. Romano, A. Raponi, D. Marchisio, M. Ciofalo, A. Tamburini, A. Cipollina, G. Micale, Analysis of particles size distributions in Mg(OH)2 precipitation from highly concentrated MgCl2 solutions, Powder Technol. 398 (2022) 117106. https://doi.org/10.1016/j.powtec.2021.117106.

[53] T. Song, F. Gao, X. Du, X. Hao, Z. Liu, Removal of boron in aqueous solution by magnesium oxide with the hydration process, Colloids Surfaces A Physicochem. Eng. Asp. 665 (2023). https://doi.org/10.1016/j.colsurfa.2023.131211.